

Study of Faraday cup designs suiting multiple electric propulsion systems.

IEPC-2022-164

*Presented at the 37th International Electric Propulsion Conference
Massachusetts Institute of Technology, Cambridge, MA, USA
June 19-23, 2022*

V.Hugonnaud¹ and D.Krejci² S.Mazouffre.³
ENPULSION, Wiener Neustadt, 2700, Austria CNRS, Orléans, 45000, France

S.Zoehrer⁴, E.Bosch Borràs⁵, and N.Wallace⁶
ESTEC, Noordwijk, 2201, Netherland

Several designs of a Faraday Cup (FC) were assessed to understand their impact on the measurement of the ion current in the ion beam of two different low power electric thrusters, namely: a Field emission electric propulsion and a radiofrequency ion engine. These two thrusters are of interest because they are among the most popular in the space propulsion market. Moreover, on a more technical and scientific viewpoint, they allow the investigation of a wide range of conditions as they operate with different propellants (indium and xenon), different current densities and with ion energies from several hundreds to thousands of volts. Study outcomes show that for both thrusters the length of the FC is a key design parameter to passively mitigate overestimation of the measured ion current. Indeed, as opposed to other classical electric propulsion systems, such as Hall thrusters, measurements in the ion beam of FEEP and RF thrusters are strongly dependent on the ion-induced electron emission yield mostly due to the ion energy range (keV) at stake. The use of ion collectors made of non-standard materials with complex structure is also of great help to reduce the ion-induced electron yield. Indeed, for aluminium the yield decreases in average by $11\pm 3\%$ for the RIT and $60\pm 8.4\%$ for the FEEP depending on the collector structure dimensions. Finally, the true ion current can be properly retrieved with the right FC architecture where secondary electron emission effects are completely counter balanced.

I. Nomenclature

η_p	=	Probe collection efficiency
$FEEP$	=	Field emission electric propulsion
γ_{EE}	=	Ion-induced electron yield
γ_{LEE}	=	Length dependant ion-induced electron yield
I_i	=	Ion current
$IIEE$	=	Ion-induced electron emission
$I_{i_{int}}$	=	Ion current integrated
RIT	=	Radiofrequency ion thruster

¹Technology expert, Engiennering, valentin.hugonnaud@enpulsion.com.

²CTO, david.krejci@enpulsion.com.

³Director of reasearch, ICARE, stephane.mazouffre@cnrs-orelans.fr.

⁴Research fellow associate, TEC, zoehrer@estec.com.

⁵Electric Propulsion Engineer, TEC-PM ,eduard.bosch.borras@esa.int.

⁶Senior Electric Propulsion Engineer, TEC-M, neil.wallace@esa.int.

II. Introduction

For the last ten years low-power electric propulsion technologies have matured and, nowadays many products are available to provide agile solution for the small satellite market. Low-power EP technologies differ from each other by their operation principle, plasma properties (ion energy, current densities, electron parameters) or propellant (noble gases, ionic liquids and metals) [1, 2]. Such a diversity introduces an issue upon standardization procedures needed to characterize the ion beam, or the plume, of thrusters. The latter can be studied by mean of plasma diagnostics. Many instruments and techniques exist but very little are cost-effective, easy to implement, providing reliable outputs while suitable for standard procedures. Within electrostatic probe types different probe architectures are available. However all rely on the same principle: An ion or electron current is measured by an electrode, termed collector, by applying a negative or positive voltage, respectively. Depending on the technique used to obtain the current, many plasma and thruster parameters can be obtained such as, ion and electron density, temperature, beam divergence, beam direction, thrust, or ionization efficiency. Amongst this type of diagnostics a Faraday cup is a powerful tool as it can be used to retrieve most of these parameters.

The main objective of this work is to discuss the possibility to build a Faraday cup enabling reliable ion current measurements from different EP systems, a RIT and a FEED in this case study. These EP technologies present similarities in term of ion energy range (keV-range). However, they differ by the propellant nature (xenon vs indium) and the current densities. FC measurements are sensitive to these phenomena as they are involved in charge exchange collisions (CEX), ion-induced electron emissions (IIE), sputtering and material deposition. Three design parameters are studied here: 1) the probe aperture diameter, 2) the ion-induced electron emission (IIEE) from different material type and structure and 3) the probe length. In this study the FEED is a laboratory unit of the ENPULSION NANO thruster commercialized by ENPULSION [3–5]. The RIT is a low-power GIE source owned by ESA. For confidential purposes no further details on the GIE source will be included.

III. Experimental apparatus

A. FEED thruster

FEED thruster experiments were conducted inside a cylindrical stainless-steel vessel of 0.91 m in diameter and 1.75 m in length located at the aerospace engineering's department laboratory of Wiener Neustadt University of Applied Sciences (FH Wiener Neustadt). Without gas injection, the pumping system allows the residual pressure in the tank to go down to 10^{-7} mbar. During operation of the FEED thruster the pressure level is typically 4×10^{-6} mbar. Since the chamber is meant to host FEED thrusters, additional care must be taken regarding materials inside the chamber. Therefore, a 1.32 m long cylindrical aluminium shield is installed inside the chamber to minimize the back flow of indium atoms during operations. It reduces the nominal diameter of the chamber down to 0.67 m. Deflectors with a sawtooth shape are installed at the back of the chamber to minimize the probability to have ions being directly backscattered towards the thruster during operation.

The probe is installed on an aluminum rotating arm. The structure allows automatic alignment of the probe with the thruster equatorial plane. The probe holder is mounted on a URS1000BCC motorized rotation stage from Newport controlled from the atmospheric side. The thruster centreline is referred to as the 0° angular position. The pivot point of the rotating structure is aligned with the thruster exit plane. The system enables a scan from -90° to $+90^\circ$ on the horizontal plane that includes the thruster axis. The alignment of the system is done thanks to a laser cross (*TOOLCRAFT CL12*). The distance d between the probe aperture and the thruster exit plane is 26.1 cm. As $d \gg d_{emitter}$ the point source hypothesis is valid [6–8]. The entire mechanical structured is grounded. The whole experimental set-up is displayed in figure 1.

A calibrated Keithley 2050 sourcemeter is used to measure the ion current collected by the probe. The device can be operated from 20 mV to 200 V in voltage source and measures 10 nA to 1 A with 0.012% basic measure accuracy. For simultaneous direct current measurement on different probe parts a Keithley 2410 is coupled to the previously mentioned sourcemeter. It offers a broad range of currents [1 A – 10 pA] and voltages [± 1100 V - ± 1 V] with a high degree of stability and accuracy.

A home-made program is used to synchronize all devices, to enable position control and to record and save measured data. Note that all current density angular distributions cover a circular arc from -90° to $+90^\circ$ with a 2° step. The current is averaged from 10 consecutive measurements acquired over 15 seconds at each angular position.

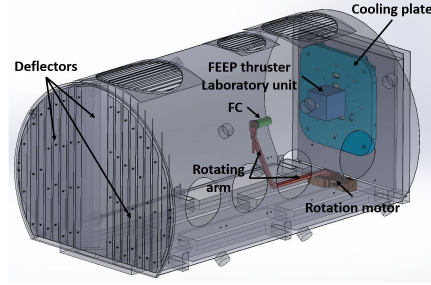


Fig. 1 3-D model of the FEED experimental apparatus in the FH chamber.

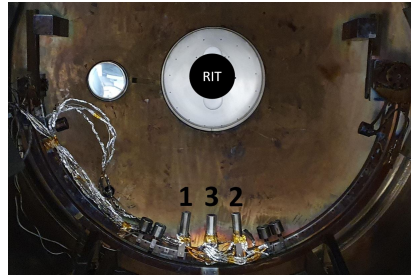


Fig. 2 Experimental apparatus used at ESTEC in the GIGANT chamber. Location 1 and 2 are $\pm 7.2^\circ$ off-centre. Probe are located 63 cm from the rotation axis of the arm. The latter is 30 cm upwards the thruster exit plane.

B. Low-power RIT thruster

The thruster is operated with xenon for our case study and the total ion acceleration is 2 kV with a total ion current (i.e., leaving the EP system) of 14.5 mA. For confidential reason no further details of the GIE source will be given. Tests were performed in the Netherlands at the ESTEC electric propulsion laboratory [9]. The test campaign was conducting in the GIGANT vacuum chamber. It is 1.6 m wide and 2.5 m long. Its pump capacity allows to reach a residual background pressure of 10^{-7} mbar during the thruster operation. A mechanical arm is installed 95 cm away from the thruster exit plane. Due to short allocated time dedicated to this test campaign we optimized the number of design parameters to be tested. We conducted two vacuum cycles where design parameters were changed in between. Also, for each cycles three probes were installed on the boom as indicated in figure 2. We labelled the probe locations 1 (left), 2 (right) and 3 (middle). Each slot was used to assess one design parameter, so three in total. In slot #1 we examined the effect of a foam #1 and flat aluminium collector material. In location #2 we examined the impact of the probe inlet diameter when it is either 3 mm or 7 mm. Finally, in slot #3 we characterized the influence of the cup length on the integrated ion current. Probes are either 50 mm or 30 mm in length.

C. Probe designs

Faraday cups are one of the most suitable electrostatic probe to be used to measure the ion beam properties for different electric thruster technologies. A Faraday cup (FC) seems to be an ideal candidate as it greatly mitigates the sheath effect during ion current acquisitions, it can be cost-effective, easy to implement and its working principle provides some degree of freedom to modify the design baseline [10, 11]. A FC is composed of three main components as shown in figure 3. The pod or housing (A) is grounded and shields electrons from the ambient plasma. The collector (C) is used to collect the ion flux penetrating inside the probe. The collector is subject to heavy ion bombardment and sensitive to subsequent ion induced electron emission as it will be discussed in next sections. The collector diameter is 12 mm for all Faraday cup designs studied in this work. Between the housing front and the collector top an electrode is inserted (B). In the literature it is designated as a "collimator", however to avoid wording confusion with "collector" the term "repeller" is used instead. Historically, the repeller is used to define the ion flux entering the probe. Therefore, it needs to have the smallest orifice diameter of the system. It screens thermal electrons and acts as a filter for ion velocity vectors. In this manner, it avoids saturation of the measurement chain when the FC is placed in the centre of the ion beam. It needs to support high level of stress such as heating, pulverization, deposition. Its role as well as its position is

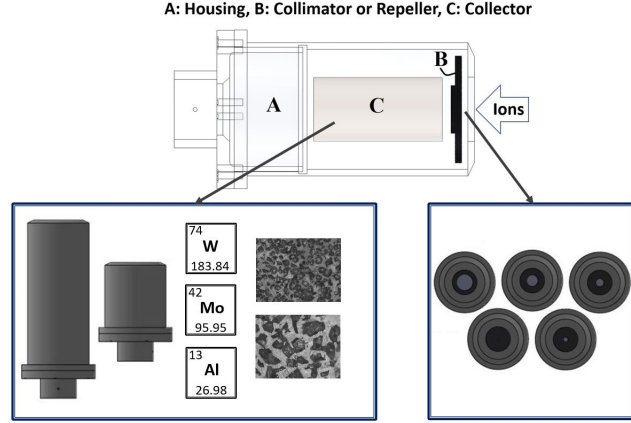


Fig. 3 Probe designs.

Table 1 Description of the foam materials commercialized by Exxentis [12].

Parameters	F1	F3	F4	F6
D_{max} (mm)	0.2 - 0.35	0.4 - 0.63	0.4 - 1.0	0.63 - 1.6
D_{min} (μm)	40 - 50	70 - 90	150 - 200	500 - 600
Volume porosity (%)		55-65		
Density (g/cm^3)		1 to 1.2		
Operating temperature ($^{\circ}\text{C}$)		from -200 to +250...550		
Aluminium alloy		AlSi7Mg		

discussed in sections V and VI. Polyetheretherketone (PEEK) is used for electrical insulation. It is a thermoplastic compatible with ultra-high vacuum application which can withstand high temperatures (melting temperature is 343°C).

Figure 3 shows the three design parameters tested 1) the probe length, 2) the collector material, 3) the collector structure and 4) the probe aperture diameter. Regarding 1), probe with cup length of 50 mm, 30 mm and 10 mm are used. For 2), materials studied are widely used by the electric propulsion community when designing plasma diagnostic: aluminium 2017A, molybdenum, tungsten and stainless steel 316L. For aluminium a foam structure is also studied with different pore sizes as can be seen in table 1. Finally, for the 4th design parameters we used aperture diameters of 10 mm, 7 mm, 5 mm, 3 mm and 1 mm. Few studies pointed out the capacity of complex surface to reduce γ_{EE} [13–16]. Materials like velvet carbon seems to be the most efficient as their body is composed of multiple nano-fibres which can ease trapping ion-induced electrons [16, 17]. Unfortunately, this type of material are exceptionally difficult to get and a foam structure was used instead, as listed in table 1.

IV. Theory

A. Plasma -probe interactions

Figure 4 presents 5 possible outcome scenarios when an ion (1) hit a surface. If not absorbed (6) by the material, the ion can be backscattered (2), induce electron emission from the material (4), provoke neutral sputtering (5) or it can also deposit (3) on the surface of the material. In the end, these processes can induce error when measuring the ion current from the ion beam of an electric propulsion (EP) thruster with an electrostatic probe [18, 19]. The magnitude of the perturbation depends on the ion source characteristics (current densities, ion energies, ion species) [20] and the composition of the target [16, 21, 22]. A part of our study will mainly focus on the ion-induced electron emission from several material types and structure when bombarding by different ion species and energies. When a neutral or charged particle reaches a surface it can induce the emission of an electron by converting its kinetic or potential energy [22–24]. This phenomena is of interest because it introduces the presence of an electron population in the measurement system which can be difficult to quantify. Indeed, the ion-induced electron yield (γ_{EE}) depends on several parameters such as angle of impact or roughness of the material surface. Moreover, the target surface undergoing an ion bombardment will

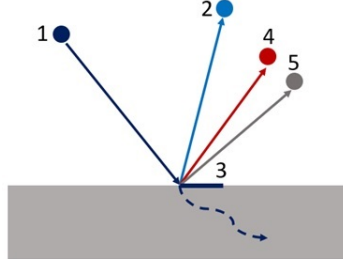


Fig. 4 Schematic of possible output from ion-surface interaction. 1) incident ion, 2) Scattered ion, 3) Neutralization and neutral ejection, 4) induced electron emission, 5) Sputtered surface material and 6) absorption or displacement.

degrade, hence the emission rate will evolve over time. The yield can be found by the ratio between the number of emitted electrons and the number of incident ions.

$$\gamma_{EE} = \frac{\text{Number of emitted electrons}}{\text{Number of incident ions}}. \quad (1)$$

Translated in terms of current it becomes:

$$\gamma_{EE} = \frac{I_{EE}}{I_{im}}, \quad (2)$$

with I_{im} the ion current and I_{EE} the induced electron current. In practice when the ion is collected by a probe and an electron is ripped off of the collector surface the absolute value of the measured current is artificially increased. Therefore, we have $I_{EE} = I_{i\&EE} - I_{im}$ where $I_{i\&EE}$ is the ion measured current including the current rise induced by EE. Equation 2 gives:

$$\gamma_{EE} = \frac{I_{i\&EE} - I_{im}}{I_{im}}. \quad (3)$$

B. Collection efficiency of the probe

The integrated total ion current $I_{i_{int}}$ can be retrieved from the ion current density angular distribution acquired in the horizontal plane that contains the thruster axis. Figure 5 displays the beam profiles acquired with a Faraday cup for a FEEP (top) and a RIT (bottom). It is clear that beams have a different current angular distribution shape. While the RIT beam profile can be assumed to be a Gaussian when the grid system used is symmetric, the other is not. The FEEP current profile can be asymmetric if the firing needles are badly distributed over the crown. Therefore, to calculate $I_{i_{int}}$, the integration method shall be compatible for all three thrusters profiles. We use cylindrical coordinates and assume symmetry of the beam around the thruster axis. We find $I_{i_{int}}$ as [25]:

$$I_{i_{int}} = \pi d^2 \int_{-\frac{\pi}{2}}^{\frac{\pi}{2}} j_i(\theta) |\sin(\theta)| d\theta, \quad (4)$$

with d the distance from the thruster to the probe, θ the angle between the probe and the thruster axis on the horizontal plane. The integration is done numerically and uses Simpson's rule.

When the ion current is known and directly controlled, like in the case of a FEEP and a RIT, one can determine the probe ion collection efficiency (η_p). If there are no ion losses during measurements then $\eta_p = 1$. It corresponds to the ratio between the integrated total ion current and the known ion current I_{em} (for FEEPs) or I_+ (for RITs).

$$\eta_p = \frac{I_{i_{int}}}{I_{em}}, \text{ or } \eta_p = \frac{I_{i_{int}}}{I_+}. \quad (5)$$

This parameter is used in this work to compare probe design outputs. There, I_{em} is averaged over 800 data points acquired during 25 minutes to mitigate small current oscillation during plume scans. I_+ is taken from the power supply display, stable over the whole experiment.

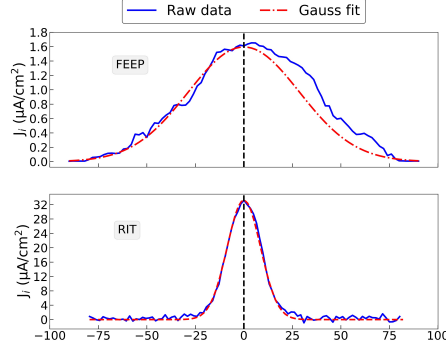


Fig. 5 Ion current density angular distribution acquired at 25 cm from a FEEP laboratory unit with 16 well distributed injectors firing at 2mA and 6 kV [18]. Bottom: The beam profile belongs to a low power RIT firing at 12.11 mA and $U_+ = 1150V$. The probe is 43 cm away from the thruster exit plane

The uncertainty accounted to calculate η_p read:

$$u = \frac{\sigma}{\sqrt{n}} \text{ or } u = \frac{\sigma}{\sqrt{3}}, \quad (6)$$

where σ is a standard deviation and n the number of acquisitions. The first equation applies if the data set has a normal distribution. If it has a rectangular or uniform distribution the second equation is preferred. All uncertainties considered are then summed up following a linear error propagation with 99% confidence level:

$$u = \sqrt{\sum_{i=1}^n u_i^2}, \quad u_{99\%} = ku \quad (k = 3). \quad (7)$$

The factor k , called coverage factor, is used here to give greater confidence that measurements are including in our tolerances [26]. Using 7 gives $u = 4\%$ with a coverage factor of 3.

V. Probe aperture dimension

The collection area used to compute I_{iint} is given by the smallest diameter of the probe assembly. The aperture diameter d_a of a FC is of great importance since it defines the ion flux flowing through the probe. Figure 6 shows the measured ion current, retrieved from a FEEP and RIT plume, by a Faraday cup equipped with different aperture diameters. At the top, values retrieved from the FEEP plume firing at 2 mA and 7 kV (blue) and 9 kV (red) are displayed. We observe a trend towards lower collection efficiencies as the aperture diameter decreases from 10 mm to 1 mm. The measured ion current is reduced by 10% by only reducing the aperture by a factor 10. We note that from 10 mm to 3 mm the decrease is around 5.3% and by only modifying the aperture from 3 mm to 1 mm the decrease is of the same order. At the bottom of figure 6 is displayed the ion current measured from a RIT plume (14.5 mA, 2 kV) by a FC equipped with either a 7 mm or 3 mm wide aperture. The same trend than for the FEEP is observed. However this time the decrease is larger. Close to 18% of loss is observed between the two configurations. When the aperture diameter is decreased it becomes more difficult to have good pointing accuracy. The error is also greater as the ion source acceleration plane is large since the ions will tend to have velocity vector non collinear to the probe axis. This phenomenon is worsened with smaller aperture diameters. Last but not least when d_a decreases it increases the probability to have ion-induced electrons from the front of the probe accelerated by the plasma sheath towards the top of the collector cup.

VI. Ion-induced electron emissions

Figure 7 displays ion-induced electron yields using equation 3 and following the experimental method described in [26]. Material studied are aluminium 2017A (a), tungsten (b), molybdenum (c) and stainless steel 316L (d) flat discs, which are widely used amongst the EP community. The plots display the evolution of their respective γ_{EE} against the mean ion energy for different emission current. Figure 7 shows that the yield increases monotonically for all materials.

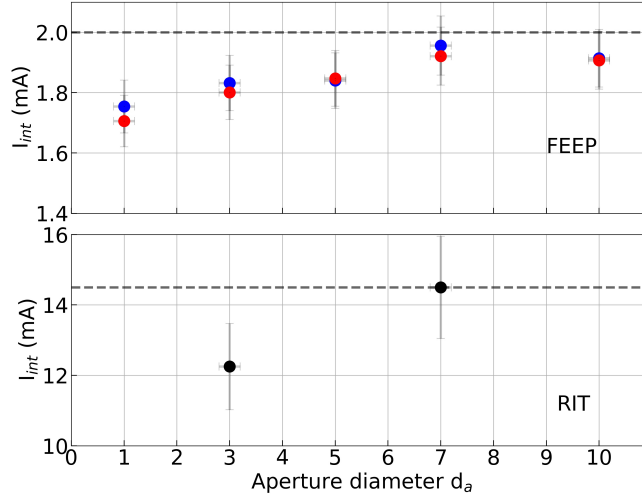


Fig. 6 Evolution of the ion current measured by a FC with different inlet apertures. Top: FEEP thruster firing with 2 mA and 7 kV. Bottom: RIT operating at 14.5 mA and 2 kV.

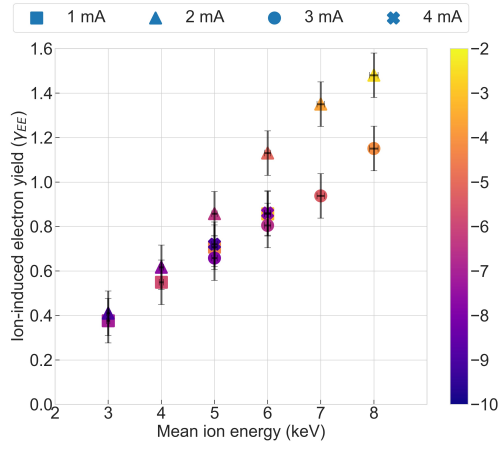
However, while the yield is of the same order for molybdenum, tungsten and steel, γ_{EE} obtained with aluminium is 3.5 to 4.5 times larger. Moreover, between the lowest and highest mean ion energy the growth rate differs for the four materials. Indeed, the rise is around 57% for molybdenum, 67% for tungsten, 72% for aluminium and approaches 95% for steel. It is noteworthy to mention that these yields are up to 2 or 3 orders of magnitude larger than data available in the literature for xenon, krypton and iodine [10, 19] as they are mostly measured at lower ion energies. In addition, in the case of an aluminium collector we note that at 2 mA the yield is getting larger than the other measured yield above 5 keV. After several measurements we saw that the behaviour keep occurring. The reason for such decoupling of the yield is still unknown as the yield should only depend on the ion energy and not on the current. For the RIT thruster, it was only possible to measure the yield for one operation point (14.5 mA and 2 kV) and only for aluminium 2017A. In that specific case γ_{EE} is 0.448. When comparing to the value displayed in figure 7 for aluminium at 3 keV ion energy we see that both yields are of the same order or magnitude.

Figure 8 shows the evolution of γ_{EE} for different aluminium collector geometries. Once more the yield increases monotonically with the bombarding mean ion energy. Here, we assume that ions entering the probe have a velocity vector purely perpendicular to the probe entrance plane. Therefore, when the angle which defines the conical shape of the collector decreases, the incidence angle (θ_i) increases. In this case, ions hit Alc with $\theta_i = 37.5^\circ$ and Alc2 with $\theta_i = 60^\circ$. We observe that increasing the incidence angle increases the yield of IIE. For higher θ_i it is easier for an ion to rip off electrons from the surface. In average, between Al (flat) and Alc the yield increases by $19.5\% \pm 3.4\%$. From Alc to Alc2 the yield increases by $14.3\% \pm 3\%$ at the highest mean ion energy.

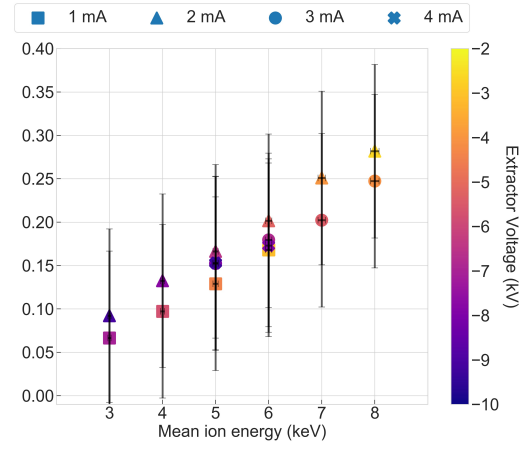
VII. Mitigation: electric fields, material structure and probe length

A. Passive mitigation

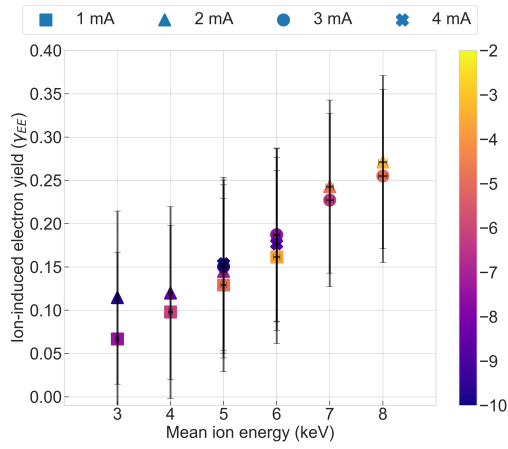
As mentioned in the previous section the effect of ion-induced electron emission is important in the case of a FEEP and RIT. Therefore, one must find a way to mitigate the artificial rise induced by those electrons on the measurement systems. In this section we propose two ways to passively reduce the impact of γ_{EE} . First by using a complex structure for the ion collector. Here we used an aluminium based foam structure. Unfortunately it was not possible to study the same foam dimensions with both thrusters units, more details are available here [26]. However the outcomes tend to show the same interpretation. Figure 9 shows the capacity of the aluminium based foam structure to reduce γ_{EE} compared to what was measured with plain aluminium (see section VI). In both cases we see that the foam structure does decreases the yield. Moreover, it is observed that the larger the pores the greater is the reduction. Indeed, γ_{EE} is reduced by 11% for the RIT with the foam #1 configuration while for the FEEP γ_{EE} goes down by 50% to 70% with the



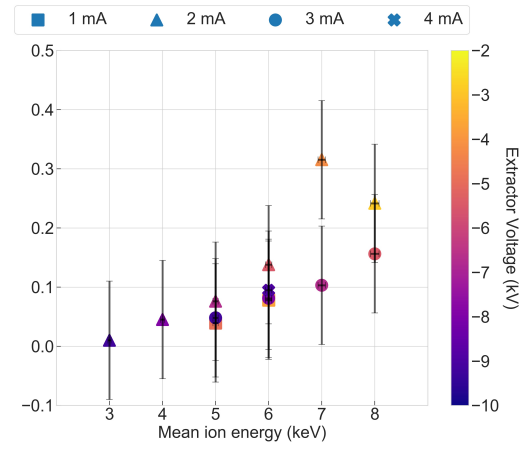
(a) Aluminum 2017A.



(b) Tungsten.



(c) Molybdenum.



(d) Stainless Steel 316L.

Fig. 7 Ion-induced electron yield (γ_{EE}) from different flat ion collector obtained with the FEEP laboratory thruster at 1, 2, 3 and 4 mA. The ion bombardment is normal to the target.

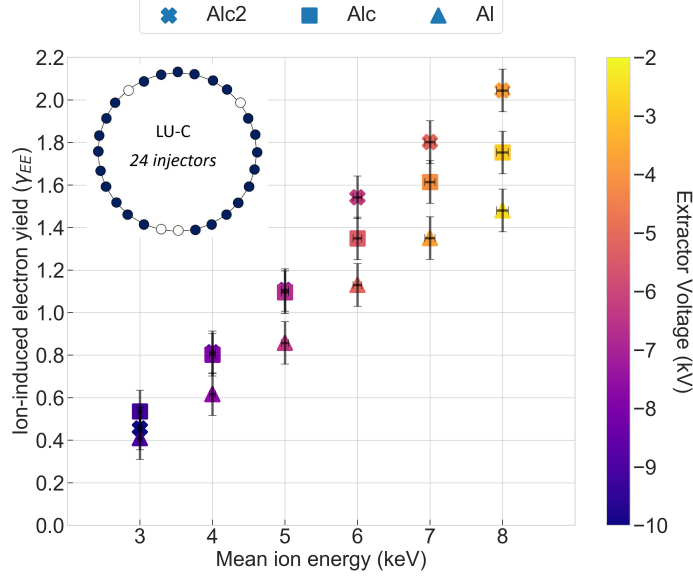


Fig. 8 Ion-induced electron yield obtained for the FEEP with different collector geometries. The thruster fires at 2 mA.

foam #6 configuration, depending on the ion energy.

A second method to decrease the artificial ion current rise measured by the probe due to electron induced emission is to scale the probe length so electrons do not manage to leave the measuring system and therefore, are recaptured. To quantify this effect we use the length dependant ion-induced electron yield γ_{LEE} . This parameter is defined as:

$$\gamma_{LEE} = \frac{I_{i\&LEE} - I_i}{I_i}, \quad (8)$$

with $I_{i\&LEE}$ the current measured by the cup when IIE reach out the probe exit.

In the case of the FEEP laboratory unit the yields are the largest for the 10 mm cup and highly dependent on the mean ion energy as can be seen in figure 10. The yield decreases when the cup length increases. Moreover, the yield is less dependant to the ion energy for larger cups. This difference could be linked to 1) the IIE energy, the more energetic the IIE the higher the probability to reach the top and 2) the IIE emission angular distribution. As the probe aperture gets closer to the rear side of the collector cup the solid angle increases and more electrons can exit the probe. At lower energy, the same trend is seen for the RIT. At 30 mm the yield is higher than 50 mm. Moreover, one can note that for 30 and 50 mm long cups the yields are of the same order for the FEEP and RIT.

B. Active mitigation: Probe length

To actively mitigate the effect of IIE on the measured ion current one can use the repeller electrode placed at the entrance of the probe as described in section III.C. The goal is to apply a bias more negative than the bias applied to the collector so electrons will be directly pushed back. With this method we enable the possibility to have small probe length as now electrons does not have time to reach the probe exit. However, as described in other publications [18, 25–27] the repeller shall not be directly exposed to the ion beam. It has to be hidden behind the probe grounded housing. This way 1) the field lines created by the repeller potential itself are better confined into the probe and 2) it is preventing accumulation of particle deposition on the repeller which can lead to short-cut with other electrodes. Figure 11 displays the ion current from a laboratory FEEP unit measured with an optimized Faraday cup using active and passive methods to mitigate perturbations induced by plasma-probe interactions. It is seen that the measured current I_{int} match (within 0.7%) with the input emitted current regardless the ion current densities and energies.

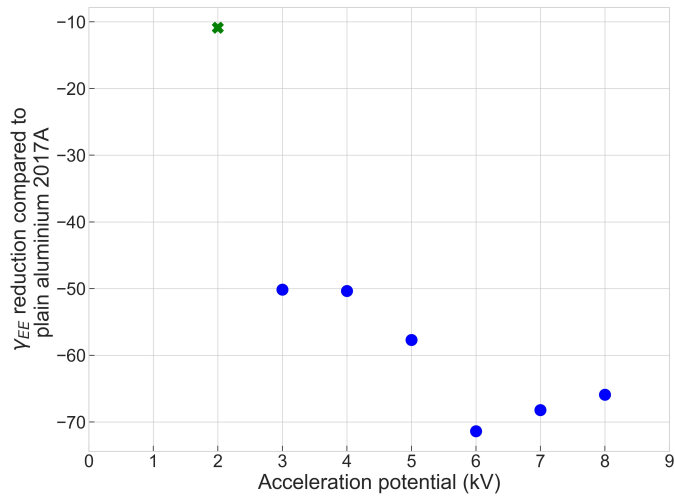


Fig. 9 Reduction of γ_{EE} when using a Foam#1 and Foam#6 structure with a RIT and FEFP respectively.

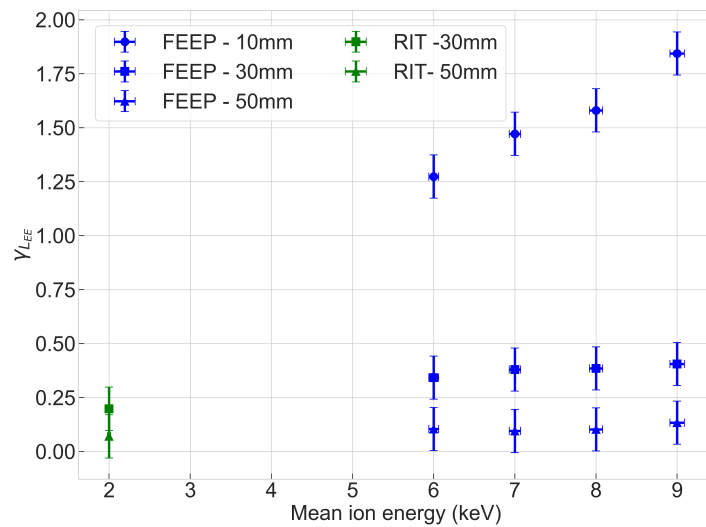


Fig. 10 Evolution of the yield of HIE exiting the probe with different cup lengths.

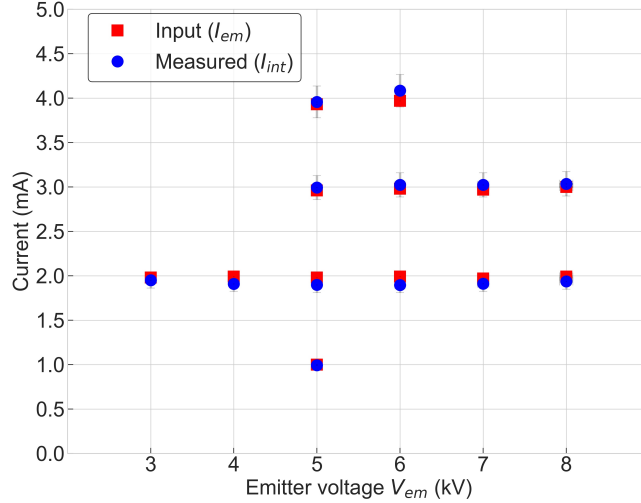


Fig. 11 Ion current measured with a Faraday cup using both passive (foam structure and 50 mm long cup) and active mitigation method.

VIII. Conclusion

In this work we were able to test several design parameters of a Faraday cup on two different type of electric propulsion systems, a FEPP and a RIT. This study is of interest as these two thrusters are to the fore in the new space market. Moreover, they have different working principles, they use different propellants, they operate with different ranges of current densities but they have ion energies of the same order of magnitude. Therefore, it was possible to scan a wide range of conditions to optimize the Faraday cup architecture to fit several case studies. It was shown that the length and aperture of the FC are of great importance. A narrower (3 mm instead of 7 mm) probe inlet could lead to underestimate the ion current by $\approx 9\%$ and 18% for the FEPP and RIT, respectively. Likewise, when studying the beam of both thrusters, one of the main perturbation is due to IIE emission. These effects can lead to largely overestimate the ion current depending on the ion energy, the material type, shape and structure. It was shown that aluminium 2017A presents the largest yield compared to molybdenum, tungsten and stainless steel 316L. We observed that a flat surface tends to emit less secondary electrons than a surface tilted with regards to the ion velocity vector. Moreover, using complex structure like foams help to reduce the yield of electrons being emitted. The larger the trapping well the higher the yield reduction. Another important driving parameter is the length of the cup. We saw that with longer cup less IIE were able to leave the cup. They were therefore recaptured and the measured current was not depending on the ion energy. This leads to only have a slight overestimation of the ion current ($\approx 5\%$) in the case of the FEPP thruster with a cup length of 50 mm without introducing additional electrodes or potential drops in the measurement system. Finally, an active way to completely mitigate IIE is to use the repeller placed at the probe entrance to push IIE back towards the collector cup. The method is highly efficient but it increases the interaction with the surrounding plasma. Therefore, it is necessary to prevent the repeller from direct exposure to the ion beam.

We showed that the impacts on the probe measurement outcomes induced by the non-identical operation parameter of a FEPP and a RIT are similar. However, the magnitude of the disturbance is not. We also seen that impact on the measured ion current cannot easily be predicted as it evolves with the current density and ion energy, hence the necessity to have the right probe architecture with the proper operation procedure.

The study presented here is part of a PhD thesis [26]. In the scope of the thesis the study was extended to a 200 W Hall thruster built by the team at ICARE-CNRS in France. HTs have radically different working principles (ionisation and acceleration phase, presence of primary electrons, CEX ions and multiply-charged ions, low and wide ion energy spectrum, random ion velocity distribution), therefore the impact on the measured ion current of all design parameters discussed here is even more important. The solution proposed here to mitigate these perturbations cannot all be applied for the HT technology.

The next steps would be to study the above mentioned design parameters for the study of the ion beam from high power electric thrusters where materials undergo higher stress. To have a clear view of the effects of each thruster on the probe design parameter one should do the experiments in an unique test facility to get rid off of external perturbations.

Acknowledgements

Authors would like to thank Dr. Scharlemann for providing the test facilities. The experiments were conducted during the PhD studies of V.Hugonnaud under the grant provided by ENPULSION. We would like to thank Dr. Aumayr from TU Wien for his advices on plasma-probe interactions. Finally, we want to thank ESA and ESTEC for providing the test facilities and the device tested over there to improve the design of our Faraday cup and adapt it for an additional electric propulsion system.

References

- [1] S.Mazouffre, “Mesure de la densité de courant ionique dans le jet plasma d’un propulseur de Hall, Expériences dans la plume du PPS1350ML,” , 2016.
- [2] D.Krejci, and P.Lozano, “Space Propulsion Technology for Small Spacecraft,” *Proceedings of the IEEE*, IEEE, 2018.
- [3] A.Reissner, N.Buldrini, B.Seifert, T.Hörbe, and F.Plesescu, “Testing and Modelling of the mN-FEEP Start-Up Performance,” *34th International Electric Propulsion Conference*, 2015.
- [4] D.Krejci and A.Reissner and T.Schoenherr and B.Seifert and Z.Saleem and R.Alejos, “Recent flight data from IFM Nano Thrusters in a low earth orbit,” *36th International Electric Propulsion Conference*, 2019.
- [5] T.Schoenherr and B.Little and D.Krejci and A.Reissner and B.Seifert, “Development, Production, and Testing of the IFM Nano FEEP Thruster,” *36th International Electric Propulsion Conference*, 2019.
- [6] D.L.Brown, and A.D.Gallimore, “Evaluation of ion collection area in Faraday probes,” *Rev. Sci. Instrum.*, Vol. 81, 2010, p. 063504.
- [7] D.L.Brown, and A.D.Gallimore, “Evaluation of facility effects on ion migration in a Hall thruster plume,” *J. Propul. Power*, Vol. 27, 2011, pp. 573–585.
- [8] T.Hallouin, and S.Mazouffre, “Far-Field Plume Characterization of a 100-W Class Hall Thruster,” *Aerospace*, 2020.
- [9] del Amo, J. G., “Electric Propulsion at the European Space Agency,” *36th International Electric Propulsion Conference*, 2019.
- [10] D.L.Brown, M.L.R.Walker, J.Szabo, W.Huang, and J.E.Foster, “Recommended Practice for Use of Faraday Probes in Electric Propulsion Testing,” *Journal of Propulsion and Power*, Vol. 33, No. 3, 2017.
- [11] S.Mazouffre, G.Largeau, L.Garrigues, C.Boniface, and K.Dannenmayer, “Evaluation of various probe designs for measuring the ion current density in a Hall thruster plume,” *35th International Electric Propulsion Conference*, 2017.
- [12] Exxentis, “Exxentis Website Homepage,” , 2017. URL www.exxentis.com.
- [13] M.Ye, Y.He, S.Hu, R.Wang, and et al., T., “Suppression of secondary electron yield by micro-porous array structure,” *Journal of Applied Physics*, Vol. 113, No. 074904, 2013.
- [14] C.Swanson, and I.Kaganovich, “Modeling of reduced secondary electron emission yield from a foam or fuzz surface,” *Journal of Applied Physics*, Vol. 123, No. 023302, 2018.
- [15] C.Huerta, M.I.Patino, and R.E.Wirz, “Secondary electron emission from textured surfaces,” *Journal Physics D:Applied Physics*, Vol. 151, No. 145202, 2018.
- [16] E.Huerta, and E.Wirz, “Ion-induced electron emission reduction via complex surface trapping,” *AIP advances*, Vol. 9, No. 125009, 2019.
- [17] A.Ottaviano, S.Banerjee, and Y.Raitses, “A rapid technique for the determination of secondary electron emission yield from complex surfaces,” *Journal of Applied Physics*, Vol. 126, No. 223301, 2019.
- [18] V.Hugonnaud, S.Mazouffre, and D.Krejci, “Faraday cup sizing for electric propulsion ion beam study: Case of a Field-Emission Electric Propulsion thruster,” *Review of Scientific Instrument*, Vol. 92, 2021.
- [19] L.Habl, D.Rafalskiy, and T.Lafleur, “Secondary electron emission due to multi-species iodine ion bombardment of different target materials,” *Journal of Applied Physics*, Vol. 129, 2021. <https://doi.org/10.1063/5.0048447>.

- [20] N.Matsunami, Y.Yamamura, Y.Itikawa, N.Itoh, Y.Kazumata, S.Miyagawa, K.Morita, R.Shimizu, and H.Tawara, "Energy dependence of the ion induced sputtering yields of monoatomic solids," *Atomic data and nuclear data table*, Vol. 31, 1940, pp. 1–80.
- [21] R.L.Petry, "Critical potentials in secondary electron emission from Iron, Nickel and Molybdenum," *Physical review*, Vol. 26, No. 346, 1925.
- [22] Baragiola, R. A., and Riccardi, P., "Critical potentials in secondary electron emission from Iron, Nickel and Molybdenum," *Reactive Sputter Deposition*, Vol. 109, 1965.
- [23] E.V.Alonso, M.A.Alurralde, and R.A.Baragiola, "Kinetic electron emission from solids induced by slow heavy ions," *Surface science*, Vol. 166, 1986, pp. 155–160.
- [24] Eder, H., Messerschmidt, W., Winter, H., and Aumayra, F., "Electron emission from clean gold bombarded by slow Au^{q+} ($q=1-3$) ions," *Journal of Applied Physics*, Vol. 87, No. 11, 2000.
- [25] V.Hugonnaud, S.Mazouffre, D.Krejci, B.Seifert, and C.Scharlemann, "Faraday cup design for low power electric thrusters," *Space Propulsion 2020+1*, 2021.
- [26] V.Hugonnaud, "Plasma Probe Measurements for Electric Propulsion Device Ion Beam: Optimization and Standardization," Ph.D. thesis, TU Wien, March 2022.
- [27] V.Hugonnaud, and S.Mazouffre, "Optimization of a Faraday cup collimator for electric propulsion device beam study: Case of a Hall thruster," *Applied Sciences*, Vol. 11, 2021.